

## Graph Theory for Fused Cubic Clusters of Water Dodecamer

Qicun Shi, Sabre Kais,\* and Joseph S. Francisco

Department of Chemistry, Purdue University, West Lafayette, Indiana 47907-1393

Received: September 5, 2005; In Final Form: October 28, 2005

The stable structures of the fused cubic water cluster  $(\text{H}_2\text{O})_{12}$  are examined using graph theoretical techniques and ab initio calculations. The calculations are obtained by scanning the symmetry of digraph structures of hydrogen-bond network spanning 12 oxygen atom vertexes. Using the Pólya theorem the cycle index expressions for 12 vertexes and 20 edges of a cuboid in point-group symmetry  $D_{4h}$  are developed. A total of 91 energy-allowed fused cubic structures are obtained, which are classified by 8 point-group symmetries: 1  $D_{2h}$ , 2  $S_4$ , 5  $C_4$ , 1  $D_2$ , 11  $C_2$ , 10  $C_i$ , 1  $C_s$ , and 60  $C_1$ . An energy level diagram of the structures reveals 14 bands that correspond to 14 unique two-colored graphs derived from the distributions of four free hydrogens of the cluster.

### I. Introduction

Water clusters, especially small water clusters, are of great interest due to their role in diverse molecular processes such as the hydrogen motion in the complex environment of bulk water,<sup>1</sup> the Serratia endonuclease dimerization in their cleavage of DNA and RNA,<sup>2</sup> the homogeneous nucleation of water into droplets and ice in radical reactions,<sup>3</sup> the coexistence of ordered surface water and crystallite-like ice structure which are dominantly cubic,<sup>4</sup> and stabilization in supramolecular self-assembly.<sup>5</sup> Moreover, small water clusters are simple examples of mathematical graphs from which information on oxygen and hydrogen connectivities are drawn.<sup>6–8</sup>

There are several studies directed at understanding the stability and geometry of the water octamer,  $(\text{H}_2\text{O})_8$ , and its other properties such as molecular potential energy models,<sup>9–15</sup> symmetry and structure,<sup>16</sup> dimerization,<sup>17</sup> thermodynamic properties,<sup>18–21</sup> hydrogen bonding topology,<sup>8</sup> and most recently, the confinement of the hydrogen molecule  $\text{H}_2$ .<sup>22</sup> Experimental studies have identified the two almost isoenergetic stable structures by infrared spectroscopy.<sup>23</sup> Some conformers have been indirectly confirmed in the study of wet electron behavior.<sup>24</sup> However, only a few studies have been performed on water dodecamer,  $(\text{H}_2\text{O})_{12}$ , concerning both energy and hydrogen bond network.

The early and relatively systematic work of dodecameric water clusters together with water octamer studied by Tsai and Jordan<sup>16</sup> applied the TIP4P model, and assigned symmetries to fused cubic structures of  $(\text{H}_2\text{O})_{12}$  isomers in a combinatorial symmetry of two octamers. Besides four tetrameric structures ( $D_{2d}2$ ,  $(D_{2d}S_4)$ ,  $(S_4)_2$ , and  $(C_{1c} C_s)$ ), there are hexameric structures, like  $S_6$  and  $D_3$ , and two cage-type structures. With the TIP4P-type potential, Wales and Hodges<sup>25</sup> searched for the global minimum of water cluster  $(\text{H}_2\text{O})_n$  ( $n = 2–21$ ), and they indicated that for  $n = 12$  the global minimum is of the fused cubic structure. For comparison with Niese and Mayne,<sup>26</sup> Wales and Hodges performed analogous runs using the TIP3P potential and showed that for  $n = 12$  the global minimum is based upon a hexagonal prism, which lies about 1.3 kJ/mol lower than the fused cube structure.<sup>26</sup>

Farantos et al.<sup>27</sup> studied water cluster  $(\text{H}_2\text{O})_n$  over  $n = 7–18$  monomers using molecular dynamics methods and an empirical potential function for many-body polarization interactions. For  $(\text{H}_2\text{O})_{12}$ , they provided two structures in the combinatorial symmetry, one from two  $D_{2d}$  octamers and one from  $S_4$  and  $D_{2d}$  octamers. The power spectra of all cubic conformations showed the low-frequency band observed in the millimeter region, indicating a possible association of stability of these multicubic clusters with the peculiar properties of liquid water.

Day et al.<sup>28</sup> searched the isomers of water clusters  $(\text{H}_2\text{O})_n$  over  $n = 6, 8, 10, 12, 14, 16, 18,$  and  $20$  with simulated annealing methods combined with the effective fragment potential and Hartree–Fock ab initio methods. For  $(\text{H}_2\text{O})_{12}$ , besides those symmetries for the four tetrameric structures mentioned above, they showed another two symmetries ( $D_{2d}C_2$ ) and  $(C_{1c})_2$ . Maheshwary et al.<sup>29</sup> considered more geometries including cuboid, fused pentagons, and fused hexagons. They found that a fusion of two cubes with  $D_{2d}D_{2d}$  symmetry (dipole moment 0) to be the most stable. A fused hexameric structure with  $S_6$  symmetry and the fused pentameric structure are less stable than the cuboids. Lee et al.<sup>30</sup> calculated the chemical binding energy of water clusters  $(\text{H}_2\text{O})_n$  ( $n = 2–20$ ) and its relation with the cluster size. The  $D_{2d}$  structures are slightly lower in binding energy than  $S_4$  structures for water clusters with 8, 12, 16, and 20 water molecules. They concluded that small water clusters composed of mainly planar four membered rings are more stable, implying the existence of magic numbers for water clusters with sizes of 4, 8, and 12.

The existence of the magic number 12 has been recently reconfirmed in the experimental studies<sup>28</sup> of dissociation pathways and energetics of  $\text{SO}_4^{2-}(\text{H}_2\text{O})_n$  for  $n = 3–17$ , where blackbody infrared radiative dissociation, sustained off-resonance irradiation collisional activated dissociation, infrared multiphoton dissociation, and double resonance are examined. The experiment showed that the  $n = 12$  cluster is more stable than either  $n = 11$  or 13. This “magic” number hydrate is consistent with filling of a shell structure at  $n = 12$ . One such structure in which all 12 water molecules are symmetrically bonded to  $\text{SO}_4^{2-}$  is identified as a low-energy structure at the B3LYP/6-31++G\*\* level,<sup>28</sup> although this structure is entropi-

cally disfavored compared to those where one or two water molecules occupy a second solvation shell.

Studies related to the water dodecamer also include an ab initio calculation by Lee et al.<sup>24</sup> using Møller–Plesset second-order perturbation theory with the TZ2P++ basis set. The most stable dodecamer is a fused cubic or tetragonal prism skeletal structure (Prism 444) with 20 hydrogen bonds (HBs). The lowest energy structure among these skeletal conformers has HB orientations with opposite helicities between adjacent tetragonal rings. In the wet electron study,<sup>31</sup> Kim et al. performed an ab initio study on an excess electron bound to the water dodecamer to determine whether the wet electron can be regarded as a precursor of the fully solvated electron. Among a number of possible geometries categorized as unbounded, surface, internal, and partially internal excess-electron states, the lowest-energy conformer is predicted to be a structure of a partially internal state.

One can see the discrete (H<sub>2</sub>O)<sub>12</sub> cluster even in the stabilization and functioning of biomolecules and in designing new materials. One example is as shown in the cavity of polymeric interlinked metallocycles of Nd(III) or Gd(III) and a podand ligand.<sup>32</sup> Different than those structures observed before, the overall structure of the water cluster can be described as an “open-cube” octamer buttressed on two sides by two water dimers. Another example is the structural variation from 1D water chain to 2D layer by varying the crystallization conditions.<sup>33</sup> The unique 2D ice layer has great similarity to ice *I<sub>h</sub>* and features a novel (H<sub>2</sub>O)<sub>12</sub> ring. The 2D structure of the water cluster is characterized through supramolecular self-assembly,<sup>34</sup> and results from the hydrogen-bonding interactions between water molecules.

Singer and co-workers<sup>35</sup> have demonstrated that graph theoretical techniques can be of considerable use in the search for stable arrangements of water clusters. Inspired by the ice rules they used graphical techniques to generate a multitude of local minima for neutral and protonated water clusters using oriented graph theory. The cubic (H<sub>2</sub>O)<sub>8</sub> and dodecahedral (H<sub>2</sub>O)<sub>20</sub> clusters and their protonated analogues are treated as examples. This idea of graph theoretical analysis of water clusters has been previously pursued by Radhakrishnan and Herndon.<sup>36</sup>

In this paper, we present a study of tetramer based (H<sub>2</sub>O)<sub>12</sub> structures via optimization in a pool of all oriented graph structures. The graph is a mathematical right square cuboid with 12 nodes, points abstracted from 12 oxygen atoms in water molecules. Our studies are motivated by the recent work of the catalytic reaction of the radical HO<sub>2</sub><sup>37</sup> in the presence of water cluster (H<sub>2</sub>O)<sub>20</sub>; and the storage of a hydrogen molecule confined in the water octamer.<sup>38</sup> In section II, the theoretical methods emphasizing the enumeration of graphs in graph theory. Section III describes the computational procedures which combine the ideas from graph theory, ice rules, and ab initio quantum chemistry methods. In section IV, the results are presented in detail for the structures, geometric parameters, and point-group symmetries of the fused cubic water dodecamer. Finally, the discussion and conclusions are given in section V.

## II. Graph Theory

Given 12 oxygen atoms, the right square cuboid we consider in the present work is prepared with three parallel and equally separated squares, top, middle, and bottom, as shown in Figure 1. The middle square may be considered a “fused” square of two squares separately from the upper cube (the top and middle squares) and the cube below (the middle and bottom squares).

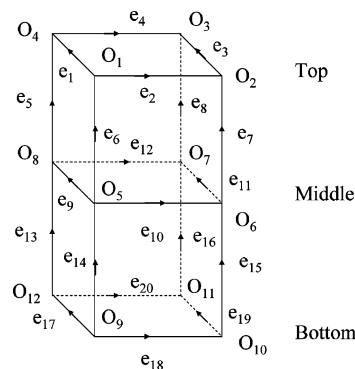


**Figure 1.** Right square cuboid with labeled vertexes and directed edges. The two orientations of each edge are binarily encoded either 1 for the up, right, and into as shown by arrows or 0 for the down, left, and out.

Each square corner is occupied by one oxygen atom. A connection between any two nearest neighboring oxygen atoms is from the hydrogen atom, which bridges one oxygen and another by a strong oxygen–hydrogen (O–H) bond and a weak interactive connection between the bonded hydrogen and remaining oxygen (H···O), i.e., forming an oxygen–hydrogen···oxygen connection (O–H···O). This is the picture developed in the previous study of smaller water clusters. In such a fully hydrogen-bonded structures there are at most 20 hydrogen bonds. The four remaining hydrogens are in free oxygen–hydrogen bond or free hydrogen bond for convenience, and hence these four hydrogens are called dangling hydrogens. Even for such a simple cuboid with the fixed position of only 12 oxygen atoms, the number of energetically favorable structures is not known. The remaining part of this paper addresses the problem concerning hydrogen covalent bonds, free hydrogen bond distributions, and their relationship with the symmetry representation of the molecular point group. To elucidate this problem, we start by examining the hydrogen bond distribution and the number of variations using graph theory.

We define an oxygen atom as a vertex of a graph, and the edge of the graph is simply a straight line which is the line connecting the two nearest neighboring oxygen atom nodes. At this time the hydrogen between the two oxygen atoms may be bound to one oxygen or another, and there are only two opposite bonding orientations for each such connections. Therefore, the graph is exactly an oriented graph with an exception that all two diagonal vertexes in any square and rectangular cycles are disconnected. The 20 bond orientations determines the number of graphs for the cuboid. The numbers of the graphs for such a partially connected and disconnected graph is less than a limit number of the general cubic, unlabeled, connected graphs<sup>39</sup> with  $2n = 12$  vertexes,

$$N_{2n,cubic} = Z^{\vee}(S_{2n}[S_3]) \cap Z^{\vee}(S_{3n}[S_2]) \quad (1)$$

The cycle index  $Z^{\vee}(S_n)$  enumerates the number of  $n$  vertexes for a symmetry group  $S_n$  by Pólya theorem<sup>40</sup>

$$Z^{\vee}(S_n) = \frac{1}{n!} \sum_p \prod_i \frac{n! x_i^{j_i}}{\prod_i k_i^{j_i} j_i!} \quad (2)$$

where  $p$  is for all partitions  $\{j_1, j_2, \dots, j_n\}$  of  $n$ , i.e.

$$\sum_{i=1}^n ij_i = n \quad (3)$$

**TABLE 1: Symmetry Groups, Ordered Energies, and Combinatorial Expressions**

no.	symmetry	order	$E^a$ (au)	$E_{\text{rel}}^a$ (au)	COS <sup>b</sup>	STE <sup>c,d</sup>	no.	symmetry	order	$E^a$ (au)	$E_{\text{rel}}^a$ (au)	COS <sup>b</sup>	STE <sup>c,d</sup>
1	$C_2$	2	-915.0148	0.0000	$(S_4)(D_{2d})$	(I'II)	47	$C_1$	1	-915.0007	0.0141		
2	$S_4$	4	-915.0143	0.0004	$(S_4)_2$	(III)	48	$C_1$	1	-915.0002	0.0141		
3	$C_2$	2	-915.0128	0.0020	$(S_4)_2$	(III)	49	$C_1$	1	-915.0002	0.0141		
4	$C_1$	1	-915.0114	0.0033	$(C_1c)'(C_s)$	(EJE)	50	$C_1$	1	-915.0002	0.0141		
5	$C_1$	1	-915.0114	0.0033	$(C_1c)(C_s)$	(BJB)	51	$C_1$	1	-915.0002	0.0141		
6	$C_1$	1	-915.0109	0.0039	$(C_1c)(S_4)$	(IEE)	52	$C_1$	1	-915.0001	0.0142		
7	$C_i$	2	-915.0107	0.0041	$(C_1c)'(C_1c)$	(EJB)	53	$C_1$	1	-914.9999	0.0145		
8	$C_2$	2	-915.0105	0.0042	$(S_4)(C_2)$	(IIA)	54	$C_1$	1	-914.9997	0.0146		
9	$C_i$	2	-915.0103	0.0044	$(C_s)'(C_s)$	(BJE)	55	$C_1$	1	-914.9996	0.0148		
10	$C_i$	2	-915.0103	0.0044	$(C_s)(C_s)'$	(EJB)	56	$C_1$	1	-914.9993	0.0150		
11	$C_1$	1	-915.0090	0.0058			57	$C_2(o)$	2	-914.9992	0.0152	$(C_1b)'(C_1b)'$	(EAE)
12	$C_1$	1	-915.0088	0.0059			58	$C_1$	1	-914.9987	0.0157		
13	$C_1$	1	-915.0085	0.0062			59	$C_2(o)$	2	-914.9986	0.0157	$(C_1b)_2$	(BAB)
14	$S_4$	4	-915.0085	0.0063	$(C_2)_2$	(AIA)	60	$C_1$	1	-914.9983	0.0161		
15	$C_1$	1	-915.0083	0.0064			61	$C_1$	1	-914.9983	0.0161		
16	$C_2(o)$	2	-915.0081	0.0067	$(C_1a)_2$	(EFE)	62	$C_1$	1	-914.9983	0.0161		
17	$C_i$	2	-915.0074	0.0074	$(C_i)'_2$	(JJJ)	63	$C_2(o)$	2	-914.9980	0.0164	$(C_4b)'_2$	(FF'F'')
18	$C_2$	2	-915.0070	0.0078	$(C_2)(D_{2d})$	(IAA)	64	$C_1$	1	-914.9980	0.0164		
19	$C_i$	2	-915.0070	0.0077	$(C_2)_2$	(IAI)	65	$C_1$	1	-914.9978	0.0165		
20	$D_2$	4	-915.0070	0.0078	$(C_2)'_2$	(IAI)	66	$C_1$	1	-914.9975	0.0168		
21	$C_1$	1	-915.0068	0.0079			67	$C_1$	1	-914.9974	0.0169		
22	$C_1$	1	-915.0067	0.0081			68	$C_1$	1	-914.9972	0.0172		
23	$C_1$	1	-915.0063	0.0085			69	$C_1$	1	-914.9970	0.0174		
24	$C_1$	1	-915.0056	0.0092			70	$C_1$	1	-914.9966	0.0177		
25	$C_1$	1	-915.0053	0.0095			71	$C_s$	2	-914.9966	0.0177	$(C_1b)'(C_1b)$	(EAB)
26	$C_1$	1	-915.0052	0.0096			72	$C_1$	1	-914.9965	0.0178		
27	$C_i$	2	-915.0043	0.0105	$(C_1d)(C_1d)'$	(FJF)	73	$C_1$	1	-914.9965	0.0179		
28	$C_1$	1	-915.0042	0.0106			74	$C_1$	1	-914.9958	0.0185		
29	$C_i$	2	-915.0041	0.0106	$(C_1e)(C_1e)'$	(FJG)	75	$C_1$	1	-914.9958	0.0185		
30	$C_1$	1	-915.0039	0.0109			76	$C_1$	1	-914.9954	0.0189		
31	$C_2(o)$	2	-915.0037	0.0111	$(C_1d)'(C_1d)'$	(JGJ)	77	$C_1$	1	-914.9950	0.0194		
32	$D_{2h}$	8	-915.0036	0.0107	$(D_{2d})_2$	(AA'A)	78	$C_i$	2	-914.9930	0.0214		(JMM)
33	$C_1$	1	-915.0029	0.0114			79	$C_1$	1	-914.9929	0.0214		
34	$C_1$	1	-915.0029	0.0114			80	$C_1$	1	-914.9927	0.0216		
35	$C_1$	1	-915.0023	0.0120			81	$C_i$	2	-914.9925	0.0218		(JLM)
36	$C_1$	1	-915.0022	0.0121			82	$C_1$	1	-914.9921	0.0222		
37	$C_1$	1	-915.0018	0.0126			83	$C_1$	1	-914.9911	0.0232		
38	$C_2(o)$	2	-915.0015	0.0129	$(C_i)_2$	(GFG)	84	$C_1$	1	-914.9905	0.0238		
39	$C_1$	1	-915.0013	0.0130			85	$C_2$	2	-914.9897	0.0246	$(C_4a)'(D_{2d})'$	II'N'
40	$C_i$	2	-915.0013	0.0131	$(C_1b)'(C_1b)$	(EAB)	86	$C_1$	1	-914.9896	0.0247		
41	$C_1$	1	-915.0012	0.0132			87	$C_4$	4	-914.9875	0.0269	$(C_4b)'_2$	(N'N'N')
42	$C_1$	1	-915.0006	0.0137			88	$C_4$	4	-914.9874	0.0270	$(C_4b)(C_4a)'$	(NNN')
43	$C_1$	1	-915.0004	0.0140			89	$C_4$	4	-914.9873	0.0270	$(C_4a)'(C_4b)'$	(NN'N')
44	$C_1$	1	-915.0003	0.0140			90	$C_4$	4	-914.9872	0.0271	$(C_4a)(C_4a)'$	(N'NN')
45	$C_1$	1	-915.0003	0.0140			91	$C_4$	4	-914.9590	0.0553	$(C_4b)'(C_4a)'$	(N'N'N')
46	$C_1$	1	-915.0003	0.0140									

<sup>a</sup> Energies are ordered in the values and increase down to the bottom,  $E_{\text{rel}} = E + 915.0148$  au. <sup>b</sup> COS: Combinatorial octamer symmetry. <sup>c</sup> STE: Stacked tetramer expression. <sup>d</sup> Key: (r) reflection in a plane crossing oxygen atoms of two water molecules and space the two covalent bond pairs either in or vertical to the plane; (') rotation of 90° about a principal axis; (") rotation of 180° about a principal axis; (o) optimized structures.

and  $i, j, k$ , and  $n$  are integers and are larger than 0. The cycle index formula for the symmetry group with  $2n = 12$  is given in Supplementary Table 1 and the graph numbers are 4379, in agreement with results by Balaban et al.<sup>41</sup> At this stage, the graph for the right square cuboid does not include the dangling hydrogens. It only shows the oxygen topology, e.g., the oxygen framework and the existence of one connection between two nearest neighboring oxygens,<sup>6</sup> and the orientation of each connection is undermined.

Next, we enumerate the number of graphs of the cuboid for a given symmetry of crystallographic point groups. The difference between the right square cuboid and the cube is that the former does not possess the  $C_3$  rotation symmetry that the latter possesses. The highest rotation operation the cuboid has is  $C_4$ . The cuboid, in a crystallographic sense, is a member of the family of tetrahedral three-dimensional objects. In this family the orders of symmetries are different, from the lowest order 4 of symmetry  $C_4$  through the highest order 16 of symmetry  $D_{4h}$ . Another rotation operation is  $C_2$ , which is in the monoclinic

and orthorhombic families with the lowest order 2 of symmetry  $C_2$  to the highest order 8 of symmetry  $D_{2h}$ .

Consider symmetry  $D_{4h}$  with the highest symmetry order, its cycle index for edges ( $e$ ) is as follows,

$$Z_{12, D_{4h}}^e(\{e_i\}) = \frac{1}{16}(e_1^{20} + 2e_1^2e_2^9 + 3e_1^4e_2^8 + 2e_1^6e_2^7 + 4e_2^{10} + 4e_4^5) \quad (4)$$

where  $e_i$  are cycle variables. Replacing  $e_i$  by  $1 + 2x^i$ , one may have the number of graphs accounted for by the edges. From eq 4 there are 67848 graphs, which show the distribution of edges or covalent hydrogen bond topology for symmetry  $D_{4h}$ . From eq 4 one can see that the number of graphs for edges decreases with the order, but increases with the number of the vertices.

Is there a way to classify the huge number of graphs? For a water molecule in the fused cubic cluster, the oxygen atom is

a donor of two hydrogens or an acceptor of at most two hydrogens. In the graph, these two bonds are either two edges or one is an edge and one a branch. All vertexes in the graph are therefore divided into two types, vertexes with a branch and vertexes without a branch. Thus, our enumerating problem of considering the dangling hydrogen distributions in the fused cubic water clusters is just the same two-color concept in graph theory. A cycle index of the vertexes has to be developed for such a graph for the two coloring problem. For a given point-group symmetry  $D_{4h}$  the cycle index of vertexes ( $v$ ) is

$$Z_{12, D_{4h}}^v(\{v_i\}) = \frac{1}{16} (v_1^{12} + 2 v_1^6 v_2^3 + v_1^4 v_2^4 + 2 v_1^2 v_2^5 + 4 v_2^6 + 2 v_2 v_{10} + 4 v_4^3) \quad (5)$$

Let  $v_i = (f + b)^i$ , where  $f$  and  $b$  are the two colors for vertexes with and without a branch, corresponding to the oxygen atoms with and without a free hydrogen connection. The cycle index expression is

$$Z_{12, D_{4h}}^v(f, b) = b^{12} + 12 b^{11} f + 66 b^{10} f^2 + 220 b^9 f^3 + 495 b^8 f^4 + 792 b^7 f^5 + 924 b^6 f^6 + 792 b^5 f^7 + 495 b^4 f^8 + 220 b^3 f^9 + 66 b^2 f^{10} + 12 b f^{11} + f^{12} \quad (6)$$

There are only four vertexes (oxygen), which have a branch (connect dangling hydrogens),  $f^4$ , and the remaining eight vertexes (oxygen) do not have a branch (do not connect dangling hydrogens),  $b^8$ . The combination of them for the cuboid produces the term  $b^8 f^4$ . From eq 6, we obtain a total of 495 unique classes of such hydrogen networks for those graphs. Here the hydrogen network is an overview of the whole cluster with all hydrogens bounded, although the orientation of hydrogens in the hydrogen bonds is not known. From the analysis above, we have a new method, using the free hydrogen bond distributions, to categorize the structure of fused cubic water clusters. We will revisit the distribution of free hydrogens in calculations in section V.

It should be emphasized that those cycle indices calculated above are based on the Pólya theorem.<sup>40</sup> It provides an upper limit to the numbers of both the oxygen topology and the hydrogen network on mathematical grounds, but it does not involve the ice rules and the way graphs are constructed.

### III. Numerical Methods

Let us start by defining the degree of a vertex. It is defined as the number of connections to all neighboring vertexes. For an oriented graph, in-degree is the number of the connections pointed to the vertex, and out-degree is the number of the remaining opposite connections. The ice rule claims that the difference between in-degree and out-degree is not larger than 1 in three-coordinate connections and is 0 in four-coordinate connections.

To construct the distinct graphs, each edge in a cuboid graph is binary encoded,  $e_i = 1$  are for up, right, and into directions and  $e_i = 0$  for down, left, and out direction as shown in Figure 1. Here  $i = 1, 2, \dots, 20$ . This binary encoding provides another upper limit of the number of all graphs for the edges of the cuboid in  $C_1$  symmetry,  $2^{20} = 1048576$ , no matter what vertex is the starting one  $i = 1$ . Figure 1 is the graph for all  $\{e_i\} = 1$ . For each  $e_i$  which is 1 or 0, its degree may be  $d_{e_i} = +1$  for into a vertex or  $-1$  for out of the vertex. Hence, for the three-coordinated vertexes in the top and bottom planes of the figure, the ice rule may be expressed in

$$-1 < d_{e_i} + d_{e_j} + d_{e_k} \leq 1 \quad (7)$$

and for the four-coordinated vertexes in the middle plane it is

$$-2 < d_{e_i} + d_{e_j} + d_{e_k} + d_{e_l} \leq 1 \quad (8)$$

Here  $i, j, k, l$  are integer indices. This rule reduces the number of graphs down to 89367 (comparable to 67848 graphs of  $D_{4h}$ ).

These 89367 graphs are categorized according to the distributive property of the net degree of 12 vertexes,  $\{O_n\}$ ,  $n = 1, 2, \dots, 12$  as labeled in Figure 1.  $O_n$  equals the sum of in-degree and out-degree for vertex  $n$ . For example,  $O_1 = d_{e_1} + d_{e_6}$  and  $O_5 = d_{e_9} + d_{e_{10}} + d_{e_6} + d_{e_{14}}$ . The number of  $\{O_n\}$  distributions,  $N_{\{O_n\}}$ , found using the ice rules is 495, which is the same as 495 by eq 6 from the Pólya theorem. The number of unique structures will be discussed in section V.

To reconstruct a graphic structure based on graph theory analysis, more information based on physical properties needs to be considered. To scan all the point-group symmetries of the dodecamer that satisfy the ice rules, the graph structures above are used as the starting point to obtain a best guess geometry. This is done by assigning specific geometrical parameters to the  $D_{4h}$  graphs, which are of the highest order in the tetrahedral family. For example, suppose the oxygen–hydrogen bond length is 0.85 Å with the hydrogen linearly targeting at a neighboring oxygen. The two neighboring oxygen–oxygen separation is 2.8 Å. The dihedral angle to fix a dangling hydrogen connecting to one of the oxygen atoms in the top and bottom planes is 33°. For the middle plane, it is 180°. The reason for starting with the  $D_{4h}$  symmetry is to construct a perfect geometry to ensure a maximal searching of the highest symmetrical structures of the cluster.

The guess geometry is used as input into the quantum chemistry optimization.<sup>42</sup> To optimize all graph structures, the semiempirical PM3 method is used initially. This is a reparametrization method of the modified neglect of diatomic overlap, MNDO, in which the AM1 (Austin model 1) form<sup>43</sup> of the core–core interaction is used. For water molecule  $H_2O$ , the PM3 gives bond length and angle 0.95 Å and 107.7° respectively, and the corresponding Hartree–Fock results (using 6-31+G(d,p) basis set throughout this paper) are 0.94 Å and 106.0°. Any of the 89367 graphs that cannot be optimized by the PM3 method are discarded. After this step, 885 graph structures are obtained. The Hartree–Fock single-point calculation is used to scan and extract all energetically unique structures, e.g., only keeping one representative for those isoenergetic structures at the Hartree–Fock level (energy numerical accuracy  $10^{-8}$  atomic units or au throughout this paper). This method resulted in 146 graphs. Next both Hartree–Fock and density functional theory methods are used to optimize the remaining structures. Frequency calculations are then performed. In the post HF calculations, the Møller–Plesset second-order (MP2) method is used to account for the electron correlation effect. At the MP2 level, 91 energetically unique structures are found.

### IV. Structures and Symmetries

**A. Overview of Geometric Structures.** In Figure 2, we show three-dimensional structures in the ball-stick representation for selected structures of fused cubic  $(H_2O)_{12}$  (all 91 unique structures can be found in the Supporting Information, Figures 1–6). The large black balls represent oxygen atoms, the small gray balls are hydrogen atoms, and the gray sticks refer to covalent hydrogen bonds. The figure inserts are arranged from

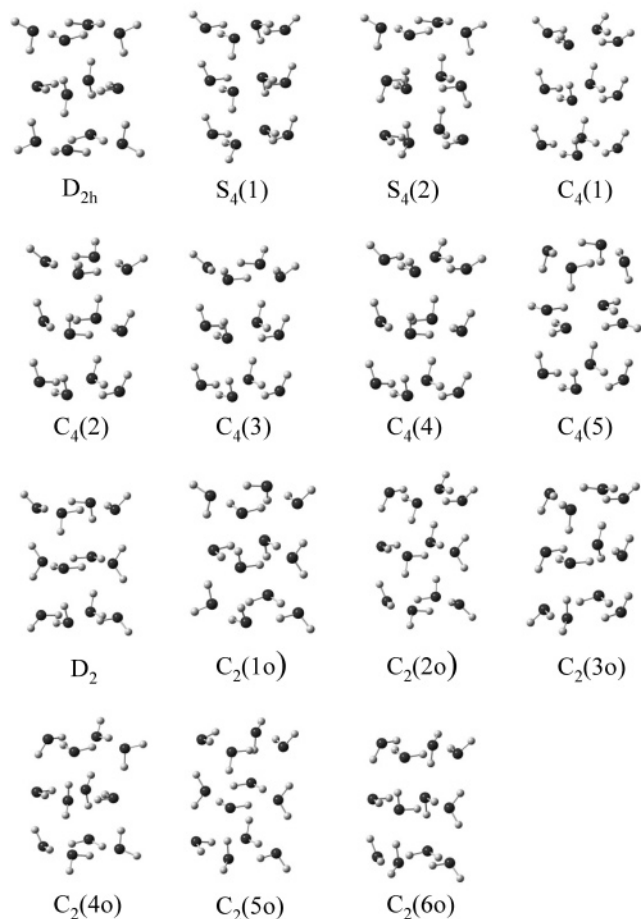


**Figure 2.** Selected fused cubic water dodecamer structures in the ball-stick representation. The large black balls represent oxygen atoms, the small gray balls are for hydrogen atoms, and the gray sticks refer to the covalent hydrogen bonds. Symmetries are  $D_{2h}$ ,  $S_4$ ,  $C_4$ ,  $D_2$ ,  $C_2$ ,  $C_i$ ,  $C_s$ , and  $C_1$ , and their symmetry orders<sup>44</sup> are 8, 4, 4, 4, 2, 2, 2, and 1, respectively.  $D_{4h}$  is removed by the ice rules. Here the principal axis of  $C_2$  is the diagonal line crossing two oxygen (o) atoms of the middle tetramer (see Figure 1).

left to right, row by row down to the bottom of a figure and grouped in terms of symmetries. In the molecular point-group representation the symmetries are  $D_{2h}$ ,  $S_4$ ,  $C_4$ ,  $D_2$ ,  $C_2$ ,  $C_i$ ,  $C_s$ , and  $C_1$ , and their symmetry orders<sup>44</sup> are 8, 4, 4, 4, 2, 2, 2, and 1, respectively.  $D_{4h}$  is removed by the ice rules.

Similarly, in Table 1, we list symmetries in columns 2 and 9, symmetry orders in columns 3 and 10, and the absolute energy values in columns 4 and 11. In columns 5 and 12, the energies for all structures are ordered starting with the lowest one. Following previous work,<sup>16,27,28</sup> a combinatorial symmetry expression is applied based on information from the water octamer case. In columns 6 and 13, we use a simpler expression in terms of stacking arrangement of the top, middle, and bottom tetramers that have several fundamental configurations shown in Figures 3 and 4. All of the energy and symmetry information are listed separately in the Supporting Information.

The electronic energy optimization compresses the graphic structures considerably by turning straight line O–H···O connection to form an obtuse angle,  $\angle\text{OHO}$ . In the O–H···O connection, O–H is the covalent bond and has an average length of 1.0 Å, 0.035 Å longer than the length of the free hydrogen bonds, 0.964 Å. The weak interactive connection, H···O, i.e., one of the hydrogens from one water molecule and the oxygen from the neighboring water molecule, has an average length of 1.896 Å, nearly two times the O–H bond length. The obtuse angle  $\angle\text{OHO}$  is approximately  $161 \pm 2^\circ$  for all structures except

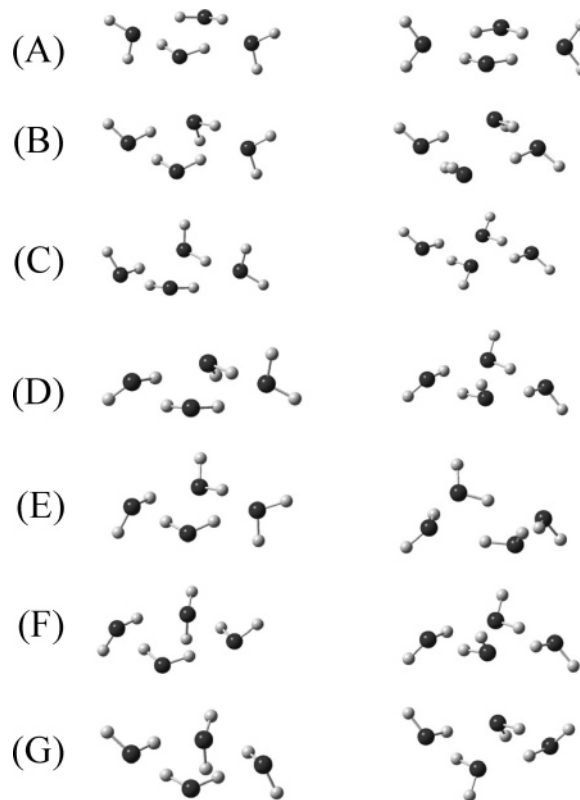


**Figure 3.** Left column: tetrameric structures which are withdrawn from optimized dodecameric structures. Right column: optimized tetrameric structures starting from the corresponding structures listed in the left column. Note that each tetramer provides at most two planes for tetramer–tetramer arrangements in dodecamers.

the one in symmetry  $D_{2h}$  where the smallest angle is  $136^\circ$ . The optimized oxygen–oxygen separations range between 2.820 and 2.850 Å is about 0.070 Å shorter than the oxygen–oxygen separation in the water dimer.

In contrast to the large variations of O–H···O connections, which may show water molecule and molecule interactions, there are minor changes in the stretching angle,  $\angle\text{HOH}$ , of a water molecule. Its average value is  $105.7^\circ$ , only  $1.4^\circ$  smaller than the gas-phase value. We also checked the angle for the three neighboring oxygens,  $\angle\text{OOO}$ . It ranges about  $\pm 3^\circ$  about  $90^\circ$  for all symmetries with an exception of  $D_2$  symmetry where the range is  $\pm 7^\circ$ . Table 2 includes all the average data within each point group symmetry.

Now, let us examine the overall characteristic of the 91 structures (See the Supporting Information). In  $C_1$  symmetry, 8 isomers labeled by  $C_1(N)$  with  $N = 22, 25, 26, 44, 46, 51, 53,$  and  $58$ , are composed of two loosely interacting water dimers and a disturbed cubic water octamer. The remaining 83 isomers are of cuboidal structures. For some of them, particularly those with  $C_s$ ,  $C_i$ , and  $C_1$  symmetry, one can see turns at the fusing plane, translations between top and bottom tetramers, and obvious changes in shape comparing them with water octamers.<sup>38</sup> As a contrast, each of the top, middle, and bottom tetramers in all 83 isomers almost maintains a planar shape. These distinctions emphasize both the fusing connection between two shaped octamers and the stacking arrangement among three tetramers.

In Figures 3 and 4, we show the tetramers structures which can be classified into three types according to the connectivity of oxygen sites and dangling hydrogens, i.e., the four hydrogen atoms are equivalently shared by two diagonal oxygen atoms, given in part A in Figure 3; shared by three oxygen atoms in

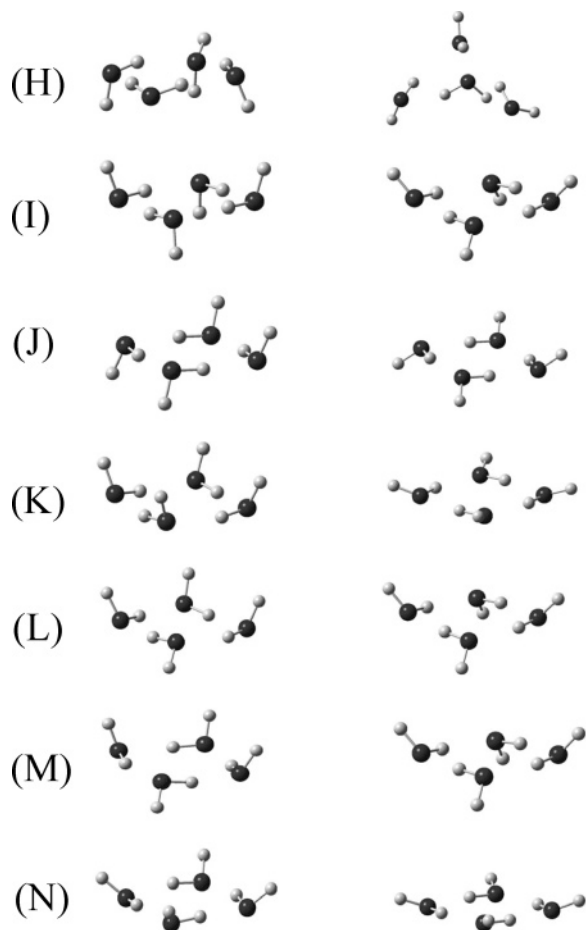


Figure 4. Continuation of Figure 3.

TABLE 2: Average Values of Geometric Parameters in Each Point-Group Symmetry

symmetry	$L_{\text{OH}}^a$	$L_{\text{OH}}^f{}^b$	$D_{\text{OO}}^c$	$\angle\text{HOH}$	$\angle\text{OHO}$	$\angle\text{OOO}$
$D_{2h}$	0.964	0.984	2.834	106.531	155.125	88.742
$S_4$	0.991	0.964	2.823	105.444	159.180	92.759
$C_4$	0.983	0.965	2.896	104.912	163.931	90.066
$D_2$	0.992	0.965	2.820	105.898	162.812	97.335
$C_2(o)^e$	0.991	0.964	2.837	105.760	160.975	93.648
$C_2^d$	0.991	0.964	2.835	105.719	160.192	90.001
$C_i$	0.999	0.964	2.840	105.296	161.934	93.216
$C_s$	0.994	0.965	2.851	106.123	162.011	89.814
$C_1$	1.017	0.963	2.847	105.374	162.321	93.114

<sup>a</sup>  $L_{\text{OH}}$ : Length of the covalent hydrogen bond in an oxygen–hydrogen  $\cdots$ oxygen connection. <sup>b</sup>  $L_{\text{OH}}^f$ : Covalent bond length between a dangling hydrogen and an oxygen atom. <sup>c</sup>  $D_{\text{OO}}$ : Distance between two oxygen atoms in an oxygen–hydrogen  $\cdots$ oxygen connection. <sup>d</sup>  $C_2$ : A 2-fold rotation group with its principal axis across the center of three tetramer planes. <sup>e</sup>  $C_2(o)$ : A 2-fold rotation group with the principal operation axis across two diagonal oxygen atoms of the middle tetramer (Figure 1).

two neighboring lateral sides, parts B–H; and one-to-one shared by the four oxygen atoms, parts I–N. These unoptimized tetramers are listed in the left-hand column of Figures 3 and 4.

In Figures 3 and 4, we also list the optimized tetramers in the right column. One will see that only the tetrameric structures A, I, J, K, and N energetically maintain the unoptimized spatial configurations of the atoms. Tetramers B, C, D, E, F, G, L, and M are not stable and transfer to stable configurations that are the optimized results of tetramers I, J, and K. The exception is tetramer H, which changes to a nontetrameric structure. For tetramer A, each oxygen shares two dangling hydrogens while

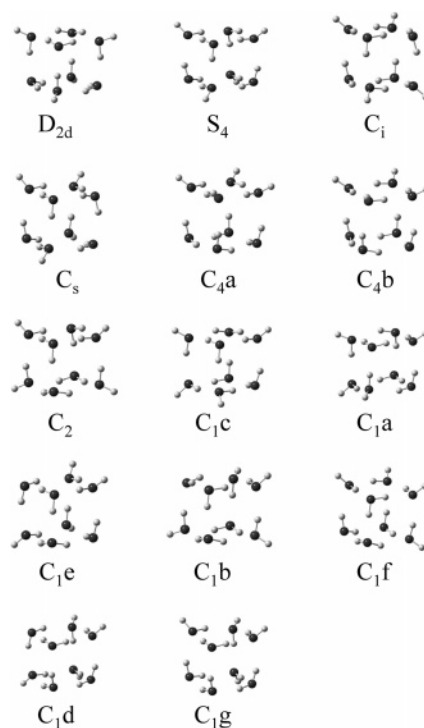


Figure 5. The 14 structures of the cubic water octamers. Note that each cube provides three orientations and at most six tetrameric planes for fusing two octamers.

in other tetramers, I, J, K, and N, one oxygen holds one dangling hydrogen. Tetramers K and N are different in the chirality of hydrogen bonds of their tetrameric rings. In tetramer I, two equally oriented dangling hydrogens are diagonal, but in tetramer J they are lateral.

### B. Symmetry for the First 10 Ground-State Structures.

In the 91 unique structures, there are 31 symmetrical structures and 60 nonsymmetrical structures (see Figures 1–6 in the Supporting Information). For example,  $C_4(2)$  is assigned to a structure that possesses  $C_4$  symmetry with the second low energy level in the symmetry. Table 1 shows the ground-state energy for all isomers with symmetry information. In the following, a detailed description is given of the symmetries for the first 10 structures, which are of the lowest energies. Their point group symmetries are  $C_2$ ,  $S_4$ ,  $C_i$ , and  $C_1$ . We then complete this section with details of the structures for the remaining symmetries  $D_{2h}$ ,  $C_4$ ,  $D_2$ , and  $C_s$ .

Before the structures and symmetries are described, it is important to mention that using a set of the tetramer-based labels do not produce symmetry information but supplement more fundamental information on stacking arrangements. The stacking arrangement information is important in constructing larger fused cubic clusters. As indicated before, the turns and relative translation between two tetrameric planes are observed in dodecameric (see Supporting Information) and even octameric structures (Figure 5). Table 1 provides the combinatorial symmetry expressions and three tetrameric arrangements in columns 6 and 7 (and columns 13 and 14) for all structures with symmetry orders larger than 1. The structures and the corresponding symmetries for the first 10 lowest energies are analyzed. Moreover, within each mentioned symmetry the remaining structures are introduced.

$C_2$  symmetry has an order of 2 and can be divided into two types according to the principal axis direction, one with its axis across the centers of three tetramer planes, and another with the axis across two diagonal oxygen (o) atoms of the middle

tetramer. We keep  $C_2(N)$  for the first and apply  $C_2(\text{No})$  for the second, where  $N$  is the index. There are five structures in  $C_2(N)$  and six structures in  $C_2(\text{No})$ .

In the  $C_2$  symmetry the five structures are  $C_2(1)$ ,  $C_2(2)$ , ...,  $C_2(5)$ . The  $C_2(1)$  structure has the lowest energy  $-915.0148$  au over all 91 structures. The energy value is listed in the first row, column 4 in Table 1. For simplicity, one may consider this isomer as two fused octamers of one  $S_4$  and one  $D_{2d}$  and both share tetramer I (as shown in Figure 4), though here  $S_4$  and  $D_{2d}$  octameric structures are not respectively equivalent to the optimized octamers in Figure 5. According to the previous work,<sup>16,27,28</sup> its combinatorial symmetry is expressed in  $(D_{2d})(S_4)$ . Viewed alternatively, this isomer includes the top, middle, and bottom tetrameric layers via four hydrogen bonds between the top and the middle and another four bonds between the middle and the bottom. With the labels given in Figures 3 and 4, we order the top, middle, and bottom tetramers in parentheses, so then the  $C_2(1)$  structure is I'II. Here the  $r$  over tetramer I means a reflection in a plane perpendicular to the tetramer plane and crossing the oxygen atoms of two diagonal water molecules. For the tetramer, this reflection operation is also equivalent to an operation reversing the chirality of a ring defined by four oxygen to hydrogen connections. It is the reflection that the chirality of the top tetramer is different from that of the middle and bottom tetramers and that the whole  $C_2(1)$  structure is of a net dipole moment 0.0017 D or 0.0007 au along its principal axis.

The second lowest energy is from  $C_2(2)$  symmetry which may be stacked with two  $S_4$  octamers,  $(S_4)_2$ , or three I tetramers, III. It has an energy of  $-915.0128$  au as given in the third row in Table 1, higher than the energy of  $C_2(1)$  by 0.0020 au or 1.24 kcal/mol. The structure has a net dipole moment along the principal axis, 0.46 D or 0.18 au, 250 times larger than that of the  $C_2(1)$  structure. The third lowest energy is given on the eighth row in column 4, Table 1, and is of symmetry  $C_2(3)$ . Its energy is  $-915.0106$  au and the dipole moment 0.28 D. Its combinatorial expressions are  $(S_4)(C_2)$  and IIA. The remaining two structures in  $C_2$  symmetry are  $C_2(4)$ , which is simply expressed in  $(C_2)(D_{2d})$  and IAA, and  $C_2(5)$  in  $(C_{4a})(D_{2d})^r$  and II'N'. Here  $r$  over an octamer also means the reflection in a plane crossing the oxygen atoms of two diagonal water molecules as defined before for the tetramer case, but the two oxygen atoms are not coplanar. The reflection plane is oriented by two lines joining the two hydrogen atoms in each of the water molecules. The two lines are either vertical to the plane or one of them in plane and another vertical to the plane. For simplicity we use  $r$  for one of the six reflection planes in the octameric cube.

$S_4$  symmetry has an order of 4. There are two unique structures for this symmetry,  $S_4(1)$  and  $S_4(2)$ . The  $S_4(1)$  structure is of the second lowest energy level, as shown in Table 1,  $-915.0143$  au. It is higher than the energy of the  $C_2(1)$  symmetry by 0.0004 au or 0.28 kcal/mol. The total dipole moment for the  $S_4(1)$  structure is zero. Compared to each other, the  $S_4(1)$  and  $C_2(2)$  structures both apparently are of the same two stacked  $S_4$  octamers and three stacked I tetramers. However, the  $S_4(1)$  symmetry includes a  $\pi/2$  rotation followed by a reflection in the plane perpendicular to the axis of the rotation while  $C_2(2)$  symmetry includes only a  $\pi$  rotation. Hence the top and bottom tetramers in the  $S_4(1)$  structure both are symmetrically compacted, and produces a zero dipole moment along the axis. In the  $C_2(2)$  structures the top and bottom tetramers are not symmetrically compacted, which leads to an axial dipole moment.

There is also an  $S_4(2)$  structure, which is stacked by two  $C_2$  octamers,  $(C_2)_2$ , or three tetramers (AIA). It has an energy of  $-915.0085$  au, this is higher than the  $C_2(1)$  structure by 0.0063 au or 3.94 kcal/mol. All data are listed in Table 1.

$C_1$  symmetry involves a total of 60 structures and contributes a structure at the fourth lowest energy. The structure includes three stacked tetramers (EJE) or two fused octamers  $(C_1c)^r(C_s)$ . The fifth lowest energy is  $C_1(2)$  with structure  $(C_1c)(C_s)$  and its three stacked tetramers are BJB.  $C_1(1)$  and  $C_1(2)$  are structures with equal energies  $-915.0114$  au. They are enantiomeric pairs, one of them is a nonsuperimposable mirror image of the other. Here the mirror plane crosses the oxygen atoms of two water molecules, one in the top tetramer and one in the bottom tetramer. The mirror is symmetrical about the covalent bonds of each of the two water molecules. From the atom-atom connection geometries and isoenergetic property one may find other structure pairs with enantiomeric symmetry in Table 1: 45th and 46th, 49th and 50th, and 61st and 62nd. The small differences (less than  $10^{-6}$  are thought to be from numerical processes with different starting geometries).

The  $C_1(1)$  and  $C_1(2)$  structures are followed by structure  $C_1(3)$ , which is the sixth level,  $-915.0109$  au, higher than  $C_1(2)$  by 0.0035 au or 2.17 kcal/mol, and it may be seen as an IEE tetrameric stacker or  $(C_1c)(S_4)$  octameric stacker.

$C_i$  symmetry is characterized with its inversion operation. There are 10  $C_i$  unique structures and they contribute the seventh lowest energy level in Table 1. Its symmetry is  $C_i(1)$  in Figure 2. In the combinatorial expression it is  $(C_1c)^r(C_1c)$  from Figure 5 and EJB from Figures 3 and 4. If the chirality of hydrogen bonds of its middle tetramer is reversed, then another structure with higher energy is obtained. Its symmetry is  $C_i(2)$ . We designate this structure  $(C_s)^r(C_s)$  and BJE.

Furthermore, starting from structure  $C_i(1)$  and if taking an atomic reflection in a plane across the centers of two water molecules, which is in the top and bottom tetrameric planes and on the diagonal position, then structure  $C_i(3)$  is obtained, the 10th energy level. Its combining structure is  $(C_s)(C_s)^r$ , and three tetramers EJB. Hence  $C_i(1)$  and  $C_i(3)$  are of energies  $-915.0103$  and  $-915.0103$  au respectively. Although their energy difference is smaller than  $10^{-6}$  (see Table 1),  $C_i(1)$  is not an enantiomer of  $C_i(3)$  because the inversion operation is improper.  $C_i$  symmetry has seven higher energy structures. The 17th is a combination of  $(C_i)^2$  and JJJ. Results for the 19th, 27th, 29th, 40th, 78th, and 81th energy levels are given in Table 1.

**C. Symmetry for the High Energy State Structures.** The following are the structural and energetic description of the remaining symmetries,  $D_2$ ,  $D_{2h}$ ,  $C_4$ , and  $C_s$ .

$D_2$  symmetry has an order of 4. In this symmetry there is only one unique structure in a combinatorial symmetry  $(C_2)^2$  with three tetramers (IAI). Here  $(C_2)^r$  is a mirror image of octamer  $C_2$  with respect to a plane involving two pairs of oxygen atoms of two diagonal water molecules in the  $C_2$  cube. The  $D_2$  structure has an energy of  $-915.0070$  au that is the 20th level.

$D_{2h}$  symmetry is of the highest order 8 in all stable structures, but its energy  $-915.0036$  au is not the lowest. It is about 0.0112 au or 7.00 kcal/mol higher than the lowest energy  $-915.0148$  au of symmetry  $C_2(1)$ . This energy is numbered as the 32nd level. and its combinatorial structure is  $(D_{2d})_2$  as shown in the previous studies.<sup>16,27,28</sup> We also express it by three tetramers (AA'A) in which A' differs from A by a rotation of  $90^\circ$  about the principal axis.

$C_s$  symmetry has symmetry order 2. Our calculation shows that there is only one unique structure for symmetry  $C_s$  which

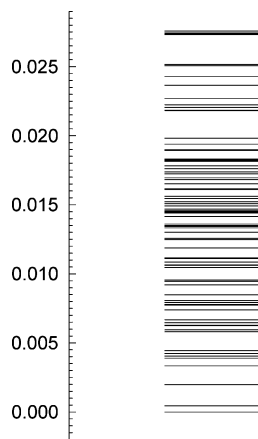


**Figure 6.** Electronic energy level (in atomic units) diagram for a reduced set of structures of fused cubic water dodecamer. Here reduced means that only one structure survives at the Hartree–Fock level of theory (see section III).

has an energy of  $-914.9966$  au, numbered as the 71th level in Table 1. The isomer includes two head-to-end octamers  $(C_1b)^r(C_1b)$  or three stacking tetramers (EAB).

$C_4$  symmetry is an interesting one since there are a total of five structures. Their energies are the highest ones at the MP2 level of theory, from the 87th through the 91st in Table 1. The 87th structure,  $C_4(1)$ , is a combination of two exactly stacked octamers  $(C_4b)_2$  or stacked tetramers  $(N^rN^rN^r)$  with an energy of  $-914.9875$  au. The following structure, the 88th, is  $C_4(2)$ ,  $0.00008$  au or  $0.05$  kcal/mol higher in energy and can be expressed in combination symmetry  $(C_4b)(C_4a)^r$  and three tetramers  $(NNN^r)$ .

If the reflection operation is made on the middle tetramer of  $C_4(1)$ , then  $C_4(3)$  structure is obtained with an energy of  $-914.9873$  au, a combinatorial symmetry  $(C_4a)^r(C_4b)^r$ , and the three tetrameric expression  $NN^rN^r$ . If structures  $C_4(2)$  and  $C_4(3)$  are compared, the expression  $(C_4b)(C_4a)^r$  is found not to be equivalent to expression  $(C_4a)^r(C_4b)^r$  because of the planar reflections and the four axially oriented dangling hydrogens. After a similar operation on the middle tetramer, one may have structure  $C_4(4)$  with an energy  $-914.9872003$  au, which are fused octamers  $(C_4a)(C_4a)^r$  and stacked tetramers  $(N^rNN^r)$ .

A structure not previously known is  $C_4(5)$  and its energy is  $-914.9590$  au, higher than that of  $C_4(4)$  by  $0.0282$  au or  $17.68$  kcal/mol. Its energy is also higher than the energy of  $C_2(1)$  by  $0.0558$  au or  $34.98$  kcal/mol, the largest energy gap for all of the structures. Each of its octamers cannot be stable, because the middle tetramer is the reflection of not a tetramer (N) but the optimized (o) one as shown in Figures 1 and 4 as well as Table 1. Its tetrameric expression may be  $N^rN^oN^r$ .

## V. Discussion

We described optimized structures of fused cube water clusters  $(H_2O)_{12}$  using combined methods of quantum chemistry calculation, graph theory, and the binary encoding technique. Our energy optimization starts with selected Pólya graphs under the ice rules. At the Hartree–Fock level of theory, we only maintain one structure and remove the remaining structures in a group of all isoenergetic structures (numerical error smaller than  $10^{-8}$  au), and hence, a reduced set of the energetically allowed structures are obtained. Figure 6 is a diagram for the energy levels of such a reduced set of unique structures. The maximal difference of energies is  $34.98$  kcal/mol.

From the energetic analysis we find that there are totally 4 enantiomeric pairs from  $C_1$  symmetry. They are expressed in

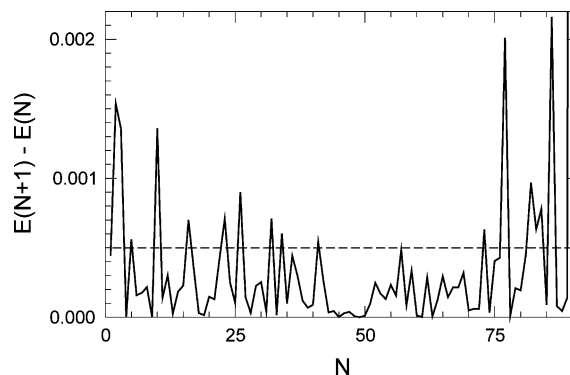


**Figure 7.** Energy difference  $E(N+1) - E(N)$  (in atomic units) as a function of the ordering index number  $N$  (see columns 1 and 8 of Table 1) with  $1 \leq N \leq 90$ .  $E(N)$  represents one of the ordered energies for the dodecamer structures.

the 9th and 10th, 45th and 46th, 49th and 50th, and 61st and 62nd levels in Table 1. Considering the real energy levels are more complex than Figure 6, we expect more enantiomeric pairs in the real energy levels; and therefore, a robust optically active property from the dextrorotatory isomers and levorotatory isomers in the water dodecamer.

Checking Figure 6 carefully, the lines of the energy levels are found to have some specific distributions: after a large space, the separation of the lines becomes small and such lines become dense until a new space appears. This observation confirms the distributions of classes of structures given in the graph theory in section II. To examine the distribution of the structures, the energy differences between two neighboring structures is calculated and listed in Table 1 and shown in Figure 7. The peaks indicate the energy level distributions. A higher peak indicates a larger space between two neighboring lines or levels. The distance between two neighboring peaks approximately defines a band. If we choose the energy difference between two neighboring levels to be larger than  $0.0005$  au, then a total of 14 bands is obtained. A relation is expected between these 14 energy level bands with the distributions of the four free hydrogen bonds. Using graph theory and quantum chemistry we have identified that there are seven classes for water octamer.<sup>38</sup> If considering the dodecamer is a combination of a cube and another tetramer based on Redfield's graph reduced function,<sup>45</sup> and if the dangling hydrogen atoms distribute in the way to minimize the Coulomb repulsion among them, then we have a total of 14 classes.

In symmetrical structures we noticed that some structures with  $C_4$  symmetry are oriented by the free covalent hydrogen bond atoms, though the maximal difference of their energies is high (up to  $0.2687$  au or  $168.63$  kcal/mol). The high energy is the result of Coulomb repulsions among those pseudo free hydrogen atoms, which are restricted to a small four-membered ring ( $2.77 \times 2.77 \text{ \AA}^2$ ). Those locally stable, highly symmetrical, and oriented structures might give us hints to study the conditions of water clusters and ice growth in some specific environments such as extreme atmospheric conditions and pressure confinements. From structure  $C_4(1)$ , one might obtain a number of longer gas-phase structures  $(H_2O)_{4n}$  by stacking iso-chiral tetramers. Whether or not they are stable within certain environmental conditions, all of these need further studies with more advanced calculations and larger basis sets that are limited in our current computing capacity.

In our study, 83 cuboidal structures generally maintain a fused cubic framework, and 8 structures are heavily distorted. The distorted structures may be simply seen as two loosely patterned

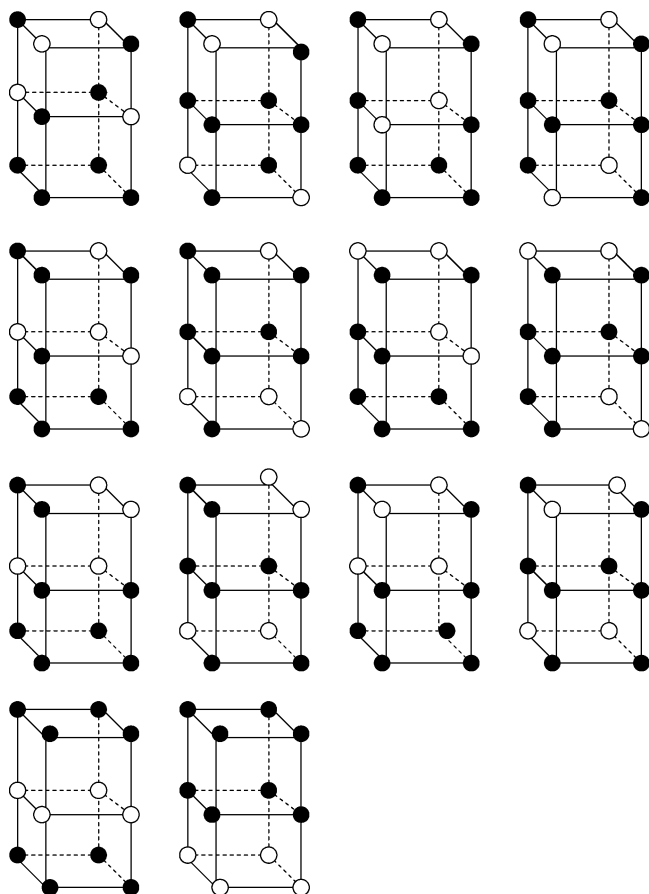


**Figure 8.** The 14 graphs with four white vertices and eight black vertices. Each white (black) vertex has (does not have) a branch.

water dimers and a disturbed cubic structure. In fact one can see more turns and translations between two tetramers for those nonsymmetric octamers and dodecamers. These indicate the possibility of other structures of water dodecameric complexes in ambient environmental conditions. These observations strongly support a recent experimental result in the cavity of polymeric interlinked metallocycles of Nd(III) or Gd(III) and a podand ligand.<sup>32</sup> The dodecameric cluster is described as an “open-cube” octamer buttressed on two sides by two water dimers and the clusters group occupy the voids in the organo-metallic framework. A more direct identification, however, should involve conformational variations over a larger pool of structures including dimeric and trimeric water components.

In summary, we have presented all energetically optimized structures of fused cube water dodecamer ( $\text{H}_2\text{O}$ )<sub>12</sub> with graph theory and ab initio calculations. Using graph theory, we have developed the cycle index expressions for 12 vertices and 20 edges in a cuboidal point-group symmetry  $D_{4h}$ , and provided the cycle index expression for the permutation symmetric group  $S_{12}$ . Our analytical and numerical enumerations confirm each other, and both set an upper limit to the numbers of graphs for optimization. A binary encoding technique has been designed in reconstructing the initial geometries of the graphs under the ice rules.

Graphs that satisfy the convergence condition in the energy using semiempirical methods (PM3) are selected for reoptimization with methods at the Hartree–Fock, density functional theory, and second-order Møller–Plesset levels using the 6-31+G(d,p) basis set. A total of 91 structures are obtained, which are vibrationally stable and distributed in 8 distinct point-group symmetries, 1  $D_{2h}$ , 2  $S_4$ , 5  $C_4$ , 1  $D_2$ , 6  $C_2(o)$  and 5  $C_2$ , 10

$C_i$ , 1  $C_s$ , and 60  $C_1$ . The diagram of the 91 structural energy levels shows 14 bands which can be mapped to 14 classes of two-colored graphs and correspond to the distributions of four free hydrogens in light of Redfield’s graph reduced function.<sup>45</sup>

**Acknowledgment.** We would like to acknowledge the partial financial support of the National Science Foundation (NSF 501 1393-0650).

**Supporting Information Available:** A table of the cycle index expression for a symmetry group with 12 vertices and figures showing water dodecamer structures with various symmetries. This material is available free of charge via the Internet at <http://pubs.acs.org>.

## References and Notes

- (1) Shin, J.-W.; Hammer, N. I.; Diken, E. G.; Johnson, M. A.; Walters, R. S.; Jaeger, T. D.; Duncan, M. A.; Christie, R. A.; Jordan, K. D. *Science* **2004**, *304*, 1137.
- (2) Miller, M. D.; Krause, K. L. *Protein Sci.* **1996**, *5*, 24.
- (3) Pfeilsticker, K.; Lotter, A.; Peters, C.; Bsck, H. *Science* **2003**, *300*, 2078.
- (4) Ruan, C. Y.; Lobastov, V. A.; Vigliotti, F.; Chen, S. Y.; Zewail, A. H. *Science* **2004**, *304*, 80.
- (5) Barbour, L. J.; William Orr, G.; Atwood, J. L. *Nature* **1998**, *393*, 671.
- (6) Anick, D. J. *J. Mol. Struct. (THEOCHEM)* **2002**, *587*, 87.
- (7) Radhakrishnan, T. P.; Herndon, W. C. *J. Phys. Chem.* **1991**, *95*, 10609.
- (8) Ojamae, L.; Shavitt, I.; Singer, S. J. *J. Phys. Chem. A* **1998**, *102*, 2824.
- (9) Kistenmacher, H.; Lie, G. C.; Popkie, H.; Clementi, E. *J. Chem. Phys.* **1974**, *61*, 546.
- (10) Stillinger, F. H.; David, C. W. *J. Chem. Phys.* **1980**, *73*, 3384.
- (11) Brink, G.; Glasser, L. *J. Phys. Chem.* **1984**, *88*, 3412.
- (12) Matsuoka, O.; Clementi, E.; Yoshimine, M. *J. Chem. Phys.* **1976**, *64*, 1351.
- (13) Kim, K. S.; Dupuis, M.; Lie, G. C.; Clementi, E. *Chem. Phys. Lett.* **1986**, *131*, 451.
- (14) Nigra, P.; Kais, S. *Chem. Phys. Lett.* **1999**, *305*, 433.
- (15) Egorov, A. V.; Brodskaya, E. N.; Laaksonen, A. *Mol. Phys.* **2002**, *100*, 941.
- (16) Tsai, C. J.; Jordan, K. D. *J. Phys. Chem.* **1993**, *97*, 5208.
- (17) Ferrari, A. M.; Garrone, E.; Ugliengo, P. *Chem. Phys. Lett.* **1993**, *212*, 644.
- (18) Wales, D. J.; Ohmine, I. *J. Chem. Phys.* **1993**, *98*, 7245.
- (19) Wales, D. J.; Ohmine, I. *J. Chem. Phys.* **1993**, *98*, 7257.
- (20) Tsai, C. J.; Jordan, K. D. *J. Chem. Phys.* **1993**, *99*, 6957.
- (21) Jensen, O.; Krishnan, P. N.; Burke, L. A. *Chem. Phys. Lett.* **1995**, *246*, 13.
- (22) Suite, B. P.; Belair, S. D.; Francisco, J. S. *Phys. Rev. A* **2004**, *70*, 033201.
- (23) Buck, U.; Ettischer, I.; Melzer, M.; Buch, V.; Sadlej, J. *Phys. Rev. Lett.* **1998**, *80*, 2578.
- (24) Lee, H. M.; Suh, S. B.; Kim, K. S. *J. Chem. Phys.* **2001**, *114*, 10749.
- (25) Wales, D. J.; Hodges, M. P. *Chem. Phys. Lett.* **1998**, *286*, 65.
- (26) Niesse, J. A.; Mayne, H. R. *J. Comput. Chem.* **1997**, *18*, 1233.
- (27) Farantos, S. C.; Kapetanakis, S.; Vegiri, A. *J. Phys. Chem.* **1993**, *97*, 12158.
- (28) Day, P. N.; Pachter, R.; Gordon, M. S.; Merrill, G. N. *J. Chem. Phys.* **2000**, *112*, 2063.
- (29) Maheshwary, S.; Patel, N.; Sathymurthy, N.; Kulkarni, A. D.; Gadre, S. R. *J. Phys. Chem.* **2001**, *105*, 10525.
- (30) Lee, C.; Chen, H.; Fitzgerald, G. *J. Chem. Phys.* **1995**, *102*, 1266.
- (31) Kim, J.; Park, J. M.; Oh, K. S.; Lee, J. Y.; Lee, S.; Kim, K. S. *J. Chem. Phys.* **1997**, *106*, 10207.
- (32) Neogi, S.; Savitha, S.; Bharadwaj, P. K. *Inorg. Chem.* **2004**, *43*, 3771.
- (33) Ma, B. Q.; Sun, H. L.; Gao, S. *Angew. Chem., Int. Ed.* **2004**, *43*, 1374.
- (34) Ghosh, S. K.; Bharadwaj, P. K. *Angew. Chem., Int. Ed.* **2004**, *43*, 3577.
- (35) McDonald, S.; Ojamae, L.; Singer, S. J. *J. Phys. Chem. A* **1998**, *102*, 2824.

- (36) Radhakrishnan, T. P.; Herndon, W. C. *J. Phys. Chem.* **1991**, *95*, 10609.  
(37) Shi, Q.; Belair, S. D.; Francisco, J. S.; Kais, S. *Proc. Natl. Acad. Sci. U.S.A.* **2003**, *100*, 9686.  
(38) Belair, S. D.; Francisco, J. S. *Phys. Rev. A* **2003**, *67*, 063206.  
(39) Harary, F.; Palmer, E. M. *Graphical Enumeration*; Academic Press: San Diego, CA, 1973.  
(40) Pólya, G. *Acta Math.* **1937**, *68*, 145.

- (41) Balaban, A. T.; Vancea, R.; Motoc, I.; Holban, S. *J. Chem. Inf. Comput. Sci.* **1986**, *26*, 72.  
(42) Frisch, M. J.; Trucks, G. W.; Schlegel, H. B.; et al. *Gaussian 98, Revision A.11.3*; Gaussian, Inc.: Pittsburgh, PA, 1998.  
(43) Herndon, W. C.; Radhakrishnan, T. P. *Chem. Phys. Lett.* **1988**, *148*, 492.  
(44) Novak, I.; *Eur. J. Phys.* **1995**, *16*, 151.  
(45) Redfield, J. H. *Am. J. Math.* **1927**, *49*, 433.